FarDU. Ilmiy xabarlar – Scientific journal of the Fergana State University

Volume 31 Issue 3, 2025-yil DOI: 10.56292/SJFSU/vol31_iss3/a215

UO‘K: 524.882

INVESTIGATING QUASI-PERIODIC OSCILLATION SIGNATURES IN THE DYONIC MODMAX MODEL USING QUASAR DATA

KVAZAR MA‘LUMOTLARIDAN FOYDALANGAN HOLDA DYONIC MODMAX MODELIDAGI KVAZI-DAVRIY TEBRANISH BELGILARINI O‘RGANISH

ИССЛЕДОВАНИЕ КВАЗИПЕРИОДИЧЕСКИХ ОСЦИЛЛЯЦИОННЫХ СИГНАТУР В МОДЕЛИ DYONIC MODMAX С ИСПОЛЬЗОВАНИЕМ ДАННЫХ QUASAR

Khoshimov Khusanboy Anvarjon ugli[1]
[1]Doctoral student at Fergana State University

Gulomov Abdujalil Abdulaziz ugli[2]
[2]Doctoral student at Tashkent State Technical University named after Islam Karimov

Abstract

In this study, we explore quasi-periodic oscillations produced near a black hole governed by the Dyonic ModMax metric. By fitting the QPO frequencies recorded from the micro-quasars GRO J1655-40, XTE J1550-564, XTE J1859+226, GRS 1915+105 and H1743-322, we establish observational limits on the charge Q and coupling γ parameters of the model. The constraints are derived through a Monte Carlo Markov Chain analysis of the data, yielding refined estimates that sharpen our understanding of black-hole behaviour within the Dyonic ModMax framework.

Annotatsiya

Ushbu tadqiqotda biz Dyonic ModMax metrikasi tomonidan boshqariladigan qora tuynuk yaqinida hosil bo‘ladigan kvazi-davriy tebranishlarni o‘rganamiz. GRO J1655-40, XTE J1550-564, XTE J1859+226, GRS 1915+105 va H1743-322 mikrokvazarlaridan qayd etilgan QPO chastotalarini moslashtirish orqali biz Q zaryadi va γ modellarining ulanish parametrlari bo‘yicha kuzatuv chegaralarini o‘rnatamiz. Cheklovlar Monte Carlo Markov Chain ma’lumotlarini tahlil qilish orqali olingan bo‘lib, Dyonic ModMax doirasidagi qora tuynuklarning xatti-harakatlari haqidagi tushunchamizni aniqlaydigan aniq hisob-kitoblarni beradi.

Аннотация

В этом исследовании мы изучаем квазипериодические колебания, возникающие вблизи черной дыры, управляемые метрикой Dyonic ModMax. Подгоняя частоты QPO, зарегистрированные в микроквазарах GRO J1655-40, XTE J1550-564, XTE J1859+226, GRS 1915+105 и H1743-322, мы устанавливаем наблюдательные пределы для параметров заряда Q и связи γ модели. Ограничения выводятся с помощью анализа данных методом Monte Carlo Markov Chain, что дает уточненные оценки, которые обостряют наше понимание поведения черной дыры в рамках Dyonic ModMax.

Key words: *Quasi-periodic oscillations, Dyonic ModMax, MCMC, RP model, lower frequency, upper frequency*
Kalit so‘zlar: *Kvazi-davriy tebranishlar, Dyonic ModMax, MCMC, RP modeli, past chastota, yuqori chastota*
Ключевые слова: *Квазипериодические колебания, Dyonic ModMax, MCMC, модель RP, нижняя частота, верхняя частота*

INTRODUCTION

The interaction between particle dynamics and quasi-periodic oscillations (QPOs) near black holes offers an exceptional probe of strong-gravity and non-linear electromagnetic effects [1-4]. Within this setting, the Dyonic ModMax framework – an extension of classical Maxwell electrodynamics that preserves dual and conformal symmetry while accommodating simultaneous electric and magnetic charges – provides a natural laboratory for testing how dyonic fields alter observable phenomena [5–7]. Instead of calculating the innermost stable circular orbit (ISCO), our study focuses directly on the observed QPO frequencies. We analyse the X-ray QPO data from the micro-quasars GRO J1655-40, XTE J1550-564, XTE J1859+226, GRS 1915+105, and H1743-322, employing a Bayesian Markov – Chain Monte-Carlo (MCMC) approach to place joint constraints on the dyonic charge parameters Q_e, Q_m and the non-linear coupling γ. The MCMC procedure yields posterior distributions that tighten the allowable ranges of these parameters and, consequently, sharpen our understanding of particle motion and radiation mechanisms in the Dyonic ModMax spacetime [8–11]. By fitting QPO frequencies alone – without an explicit ISCO calculation – we demonstrate that strong-field electromagnetic–gravitational interplay can be effectively constrained, highlighting the diagnostic power of QPOs for testing nonlinear electrodynamic extensions of general relativity.

QUASI-PERIODIC OSSILATION

In this subsection we explore the allowable ranges of the upper (vU) and lower (vL) twin-peak HF-QPO frequencies predicted by models that tie the observed signals to the fundamental epicyclic motions of particles orbiting compact gravitating sources [12-13]. We focus on the following framework:

The Relativistic-Precession (RP) model. Originally introduced by Stella and Vietri to interpret kHz twin-peak QPOs in neutron-star low-mass X-ray binaries (0.2–1.25 kHz) [14-17], the RP scheme was later shown to apply equally well to black-hole binaries. Ingram subsequently refined the model so that fits to the power-density spectrum of a microquasar's accretion disc could deliver precise estimates of the central black hole's mass and spin. Within the RP picture the twin peaks are identified with combinations of the orbital (Keplerian), radial-epicyclic and vertical-epicyclic frequencies, $\nu_\phi, \nu_r, \nu_\theta$. The vertical component, ν_θ stems from axisymmetric oscillations perpendicular to the disc plane – i.e. mild disc warping –and the model incorporates the impact of non-axisymmetric modes on the disc's dynamical behaviour around strongly gravitating objects.

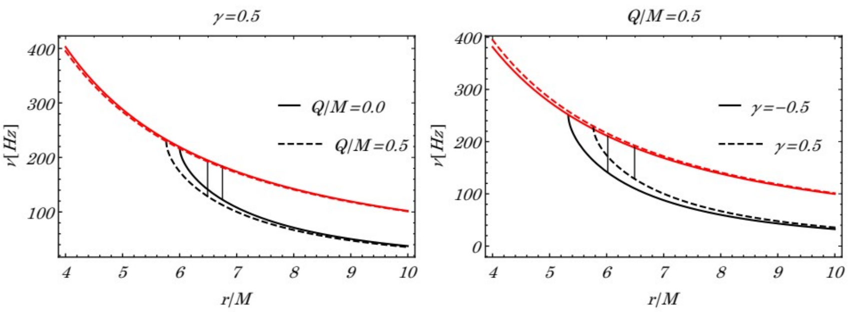

FIG. 1. The radial profile of the upper (vU, Red) and lower (vL, black) frequencies is presented for the RP model. Furthermore, r3:2 resonance radii are also displayed by solid vertical lines.

The radial dependence of the upper and lower frequencies of twin QPOs is presented in Fig. (1), with the red and black lines representing them, respectively. In the upper panel, γ is set to γ = 0.5, and Q = 0 is represented by the solid line and the dashed line for Q = 0.5. It can be seen from this panel that a decrease in both the upper and lower frequencies is caused by an increase in the Q parameter, and the QPO orbit with a frequency ratio of 3 : 2 is shifted slightly outward. In the right panel, γ = −0.5 is represented by the solid line, while γ = 0.5 is shown by the dashed line, with the parameter Q = 0.5.

Markov-Chain Monte-Carlo (MCMC) parameter inference

To translate the twin-peak QPO measurements into quantitative limits on the Dyonic ModMax spacetime, we analyse the X-ray binary systems GRO J1655-40, GRS 1915+105, XTE J1550-564, XTE J1859-226, and H1743-322. For each source we fit the Relativistic-Precession (RP) model to the observed upper (ν_U) and lower (ν_L) frequencies by means of an ensemble-sampler MCMC implemented with the MCMC Python package[18-19].

The joint posterior distribution for the parameter vector

$$P(\Theta|D,M) = \frac{P(D|\Theta,M)\pi(\Theta|M)}{p(D|M)}, \quad (1)$$

is where $\pi(\Theta)$ is the $P(D|\Theta,M)$ the likelihood, and Z the evidence. We utilize independent Gaussian prior distributions.

$$\pi(\theta_i)\ \exp\left(-\frac{1}{2}\left(\frac{\theta_i-\theta_{0,i}}{\sigma_i}\right)^2\right) \quad (2)$$

where $\Theta_{low,i} < \Theta_i < \Theta_{high,i}$ for the parameters $\Theta_i = [M, Q, \gamma, r]$, and σ_i represents their corresponding standard deviations. The previous values for the parameters of the black hole are outlined in Table (II).

Based on the upper and lower frequency data presented in Sec. IV A, our MCMC analysis is designed to incorporate two separate datasets. Central to this analysis is the likelihood function, denoted as L, which is articulated as follows:

$$\log L = \log L_{up} + \log L_{low}, \tag{3}$$

where log L_{up} denotes the likelihood corresponding to the upper-frequency data, calculated as:

$$log\, L_{up} = -\frac{1}{2}\sum_i \frac{(\nu_{i,uo,obs}-\nu_{i,low,th})^2}{(\sigma_{i,low,obs})^2}, \tag{4}$$

Conversely, log L_{low} denotes the likelihood attributed to the lower-frequency data, expressed as:

$$log\, L_{low} = -\frac{1}{2}\sum_i \frac{(\nu_{i,uo,obs}-\nu_{i,low,th})^2}{(\sigma_{i,low,obs})^2}, \tag{5}$$

Within this framework, the index i varies from 1 to an arbitrary integer, which denotes the number of detected upper and lower quasi-periodic oscillation frequencies. The frequencies identified through observation are represented as $\nu_{up,obs}$ and $\nu_{low,obs}$, corresponding to ν_{up} and ν_{low}, respectively. Moreover, $\nu_{(up)}$ and $\nu_{(low)}$ refer to their theoretical counterparts. Furthermore, $\sigma_{(up,obs)}$ and $\sigma_{(low,obs)}$ denote the statistical uncertainties associated with these measurements.

Figure 2 illustrates the resulting corner plots, where the shaded areas represent the 68% (1σ), 90% (2σ), and 95% (3σ) credible intervals for each pair of parameters. The best-fit values along with their 1 σ uncertainties are summarized in Table III; in summary:

Sources	M/M⊙	$\nu_{upper}(Hz)$	$\nu_{lower}(Hz)$
GRO J1655-40	5.4 ± 0.3	441 ± 2	298 ± 4
GRS 1915+105	$12.4^{+2.0}_{-1.8}$	168 ± 3	113 ± 5
XTE J1550-564	9.1 ± 0.61	276 ± 3	184 ± 5
XTE J1859+226	7.85 ± 0.46	$227.5^{-2.4}_{+2.1}$	$128.6^{+1.6}_{-1.8}$
H1743-322	$\lesssim 9.78$	240 ± 3	165^{+9}_{-5}

The deduced masses are grouped within the range of 5 and 12 $M\odot$ aligning with dynamical assessments. The charge parameter Q is non-zero but remains significantly below the maximum threshold in all instances, while the nonlinear coupling γ varies from approximately −0.4-0.4−0.4 to +0.2+0.2+0.2. These variations influence the local electromagnetic and gravitational fields, thereby shaping the twin-peak QPO spectrum unique to each system. In particular, the high charge of GRO J1655-40 ($Q \simeq 0.76$) amplifies electromagnetic forces in the innermost disc, while the negative γ value preferred for GRS 1915+105 modifies the effective potential, consequently enhancing the radial precession component.

TABLE II. The Gaussian prior of the Dyonic Mod Max from QPOs for the X-ray Binaries

Sources	$M/M\odot$	r/M	γ	Q/M
GRO J1655-40	5.4±0.3	5.39±0.33	0.225±0.5	0.5±0.20
GRS 1915+105	12.4±0.3	5.73±0.37	-0.4±0.061	0.50±0.12
XTE J1550-564	9.1±0.61	5.26±0.45	-0.25±0.4	0.50±0.20
XTE J1859+226	7.85±0.46	6.26±0.46	-0.4±0.4	0.05±0.15
H1743-322	9.78±0.24	5.56±0.13	0.29±0.02	0.761±0.15

TABLE III. The optimal estimates of black hole parameters derived from quasi-periodic oscillations (QPOs) for the chosen X-ray sources.

$Sources$	$M/M\odot$	r/M	γ	Q/M
$GRO\ J1655-40$	$4.667^{+0.094}_{-0.13}$	$6.16^{+0.14}_{-0.10}$	$-0.02^{+0.19}_{-0.21}$	0.534 ± 0.027
$GRS\ 1915+105$	12.35 ± 0.73	6.11 ± 0.27	-0.39 ± 0.12	$0.48^{+0.11}_{-0.09}$
$XTE\ J1550-564$	$8.16^{+0.46}_{-0.53}$	5.72 ± 0.30	$0.32^{+0.30}_{-0.35}$	$0.63^{+0.11}_{-0.12}$
$XTE\ J1859+226$	7.29 ± 0.16	7.235 ± 0.0073	-0.43 ± 0.20	0.202 ± 0.15

$H1743-322$	9.78 ± 0.24	5.56 ± 0.13	0.29 ± 0.02	0.761 ± 0.15

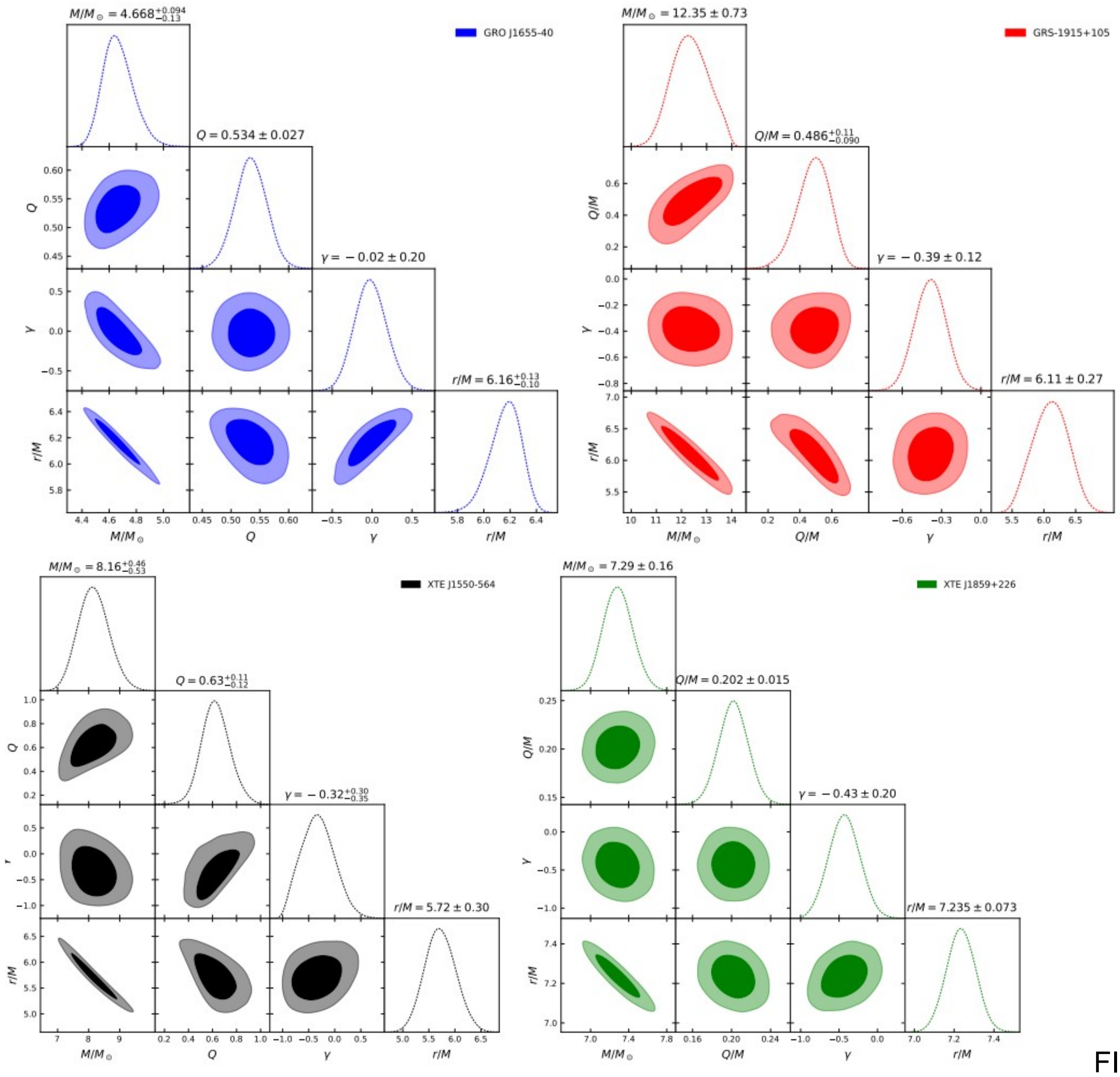

FIG.2.This figure show Constraints on the parameters of Dyonic ModMax with GRO J1655–40, XTE J1859+226, XTE J1550–564, GRS 1915+105 and H1743-322 from current observations of QPOs within the relativistic precession model.

CONCLUSION

The study examined three microquasars as candidates for stellar mass black holes. The results from the (MCMC) analysis are illustrated in Figure 2, where the shaded contours represent confidence levels of $1\sigma\ (68\%), 2\sigma\ (90\%)$, and $3\sigma\ (95\%)$ for the posterior probability distributions across the entire parameter set. This figure is divided into four panels: the upper left panel pertains to GRO J1655–40, the upper right to GRS 1915+105, the lower left to XTE 1550–564, and the lower right to XTE J1859+226. Detailed prior values for the parameters μ and σ, which characterize the distributions of the parameters M, Q, γ, and r, are listed in Table II, while their best-fit values for these objects are presented in Table III.

LIST OF LITERATURE

1. A. Maselli, G. Pappas, P. Pani, L. Gualtieri, S. Motta, V. Ferrari, and L. Stella, Astrophys. J. 899, 139 (2020), arXiv:1905.05616 [astro-ph.HE].

2. J. Rayimbaev, A. Abdujabbarov, and H. Wen-Biao, Phys. Rev. D 103, 104070 (2021).

3. A. Davlataliev, F. Atamurotov, A. Abdujabbarov, N. Juraeva, and V. Khamidov, Phys. Dark Univ. 46, 101603 (2024).

4. A. Ashraf, A. Ditta, D. Sofuo˘glu, W.-X. Ma, F. Javed, F. Atamurotov, and A. Mahmood, Physica Scripta 99, 065011 (2024).
5. J. Rayimbaev, U. Eshimbetov, B. Majeed, A. Abdujabbarov, A. Abduvokhidov, B. Abdulazizov, and A. Xalmirzayev, Chinese Physics C 48, 055104 (2024).
6. G. Mustafa, G. D. A. Yildiz, F. Javed, S. K. Maurya, E. G¨udekli, and F. Atamurotov, Phys. Dark Univ. 46, 101647 (2024).
7. G. Mustafa, E. Demir, A. Davlataliev, H. Chaudhary, F. Atamurotov, and E. G¨udekli, Phys. Dark Univ. 46, 101644 (2024).
8. A. Caliskan, G. Mustafa, T. Naseer, S. K. Maurya, E. G¨udekli, S. Murodov, and F. Atamurotov, Journal of High Energy Astrophysics 44, 99 (2024).
9. Y. Feng, A. Ashraf, S. Mumtaz, S. K. Maurya, G. Mustafa, and F. Atamurotov, Journal of High Energy Astrophysics 43, 158 (2024).
10. F. Khosravani, J. Sadeghi, and S. Noori Gashti, Pramana 98, 92 (2024).
11. M. R. Shahzad, G. Abbas, H. Rehman, and W.-X. Ma, Eur. Phys. J. C 84, 461 (2024).
12. S. Murodov, J. Rayimbaev, B. Ahmedov, and E. Karimbaev, Universe 9, 391 (2023).
13. S. Shaymatov, B. Ahmedov, M. De Laurentis, M. Jamil, Q. Wu, A. Wang, and M. Azreg-A¨ınou, Astrophys. J. 959, 6 (2023), arXiv:2307.10804 [gr-qc].
14. S. Shaymatov, M. Jamil, K. Jusufi, and K. Bamba, Eur. Phys. J. C 82, 636 (2022), arXiv:2205.00270 [gr-qc].
15. J. Rayimbaev, B. Majeed, M. Jamil, K. Jusufi, and A. Wang, Phys. Dark Univ. 35, 100930 (2022), arXiv:2202.11509 [gr-qc]. 13
16. K. Jusufi, M. Azreg-A¨ınou, M. Jamil, S.-W. Wei, Q. Wu, and A. Wang, Phys. Rev. D 103, 024013 (2021), arXiv:2008.08450 [gr-qc].
17. A. Davlataliev, B. Narzilloev, I. Hussain, A. Abdujabbarov, and B. Ahmedov, Phys. Dark Univ. 46, 101569 (2024).
18. L. Stella and M. Vietri, in 19th Texas Symposium on Relativistic Astrophysics and Cosmology, edited by J. Paul, T. Montmerle, and E. Aubourg (1998) p. 315.
19. S. E. Motta, T. M. Belloni, L. Stella, T. Mu˜noz-Darias, and R. Fender, Mon. Not. R. Astron. Soc 437, 2554 (2014).